Hybrid Advances 4 (2023) 100090

Contents lists available at ScienceDirect

Hybrid Advances

journal homepage: www.journals.elsevier.com/hybrid-advances

Bending analysis of glass fiber reinforced epoxy composites/copper-clad laminates for multi-layer printed circuit boards

Md Nazmul Islam [a], Md Sayed Anwar [b], Md Shariful Islam [a,*], Md Arifuzzaman [a], Md Abdullah Al Bari [c]

[a] Department of Mechanical Engineering, Khulna University of Engineering & Technology, Khulna, Bangladesh
[b] Department of Mechanical Engineering, Sonargaon University, Dhaka, Bangladesh
[c] Department of Chemical and Petroleum Engineering, University of Calgary, Alberta, Canada

ARTICLE INFO

Keywords:
Printed circuit board
Ply orientation
Lamina thickness
Bending properties
Finite element analysis

ABSTRACT

Printed circuit board (PCB) is the most important part of any electronic device which is made of copper-clad laminate and glass fiber-reinforced composites. Since the ply orientation of fiber-reinforced composites and lamina thickness have a significant influence on the mechanical properties of the whole composite laminate it is necessary to investigate the effects of ply orientation and lamina thickness on the bending properties of PCB so that they can be manufactured to meet the service requirements. In this work, the bending properties of PCB were investigated for seven different ply orientations of glass fiber-reinforced composite laminas and for eight different thickness combinations (for a constant laminate thickness) of glass fiber-reinforced composite lamina and copper-clad laminate. A commercially available finite element analysis software (Abaqus) was used to simulate a three-point bending test of PCBs and the simulation results were validated using experimental results. It is found that the bending stiffness is maximum for the cross-ply laminate. The introduction of angle ply improves the maximum von-Mises stress of the PCB with an insignificant cost of bending stiffness (less than 5% reduction). It is found that the bending stiffness and the maximum von-Mises stress of the PCB can be regulated through the variation of thickness of the constituent lamina. The laminate stiffness can be increased by increasing the thickness of stiffer laminas or by placing the stiffer laminas towards the surface of the laminate. The outcome of this research would provide a comprehensive understanding of the bending characteristics of the multi-layered PCBs which can be directly utilized by the PCB manufacturers. However, the effects of ply orientation and lamina thickness variation on the behavior of the PCBs subject to temperature variation, impact loading, vibration, and other conditions that might affect the service life of the PCBs should be investigated.

1. Introduction

A printed circuit board (PCB) is the heart of any electronic device and in the modern era, the use of electronic devices is increasing day by day. From cell phones to tablets, computers, laptops, and televisions are a few electronic devices that become a part of our daily life. During the service life, these devices encounter many types of loading including bending, thermal, impact, fatigue, or even vibration [1]. Ensuring the strength and durability of electronic devices is crucial to withstand the various loads they encounter throughout their service life. Among the essential components, PCBs play a significant role and must be well-protected from any external loading that might compromise their integrity. Despite its smaller thickness and size, it is imperative for the PCB to absorb and sustain these loads without failure. Therefore, an intensive study is required to enhance the properties of a PCB to meet these requirements. The major components of a multi-layer PCB are glass fiber-reinforced epoxy composites which are commonly known as FR-4 and copper foil used as copper-clad laminate (CCL) [2]. Since a multi-layer PCB contains several layers of FR-4 and CCL, their individual layer thickness plays an important role under bending load. Again, FR-4 contains glass fiber-reinforced epoxy composites. So, the fiber orientation on the FR-4 also has a significant contribution to the bending properties of a PCB.

Since different layers in PCBs have different mechanical properties, they are orthotropic in nature [3]. Hutapea and Grenestedt [4] investigated the elastic properties of FR-4/CCL laminates subjected to

* Corresponding author.
E-mail address: msislam@me.kuet.ac.bd (M.S. Islam).

https://doi.org/10.1016/j.hybadv.2023.100090
Received 20 August 2023; Received in revised form 17 September 2023; Accepted 20 September 2023
Available online 21 September 2023

different temperatures. They found that if the temperature raised to the glass transition temperature of epoxy, the shear modulus of elasticity in both in-plane and out-of-plane significantly decreased. Young's modulus in both warp and fill directions was less affected by the elevated temperature. The effect of cooling on the thermomechanical properties of PCBs is studied by Ramdas et al. [5] and they reported that Young's modulus of elasticity of FR-4 decreased after immersion cooling in dielectric fluid EC100. Kim et al. [6] developed a simulation method to predict the warpage caused by the patterning process in PCBs where they have simplified the nonlinear thermo-elasticity problem into a linear one by adjusting thermal loading. The deflection predicted by the simulation was very close to the actual deflection found in the experimental results.

Over the years, researchers have used different models for the prediction of thermo-mechanical properties of PCBs such as convolutional neural networks [7], deep learning [8], deep neural networks [9], 3-D convolutional neural networks [10], etc.

Dissimilar materials with different coefficients of thermal expansion cause warpage in the PCBs [11–18] Lee et al. [19] studied the warpage of CCL/FR-4 which occurs from the residual stress developed in the CCL during manufacturing. They have investigated the flexural modulus of elasticity and coefficient of thermal expansion for four different fiber orientations (0°, 45°, 90°, and 135°) and found that cross-ply laminates have a better modulus of elasticity compared to angle-ply laminates. Lee [20] developed a finite element model to study the out-of-plane deflection of PCBs caused by the coefficient of thermal expansion mismatch between constituent materials. Haugan and Dalsjø [21] have investigated the bending properties of low and high glass transition temperature FR-4 laminates and found that warp-4 (width = 14.07 mm, thickness = 1.59 mm and not exposed to soldering) laminate has the highest modulus of elasticity of 24.84 GPa. Chippalkatti et al. [22] investigated both numerically and experimentally the natural frequency of 5 different PCBs of different dimensions and varying CCL thickness. They have predicted the orthotropic material properties of PCBs using their experimental results as the PCBs contain both FR-4 laminas and CCL. Fellner et al. [23] studied the cyclic mechanical properties of glass fiber-reinforced composites sandwiched between copper layers. They have considered five layers of thin copper and four layers of FR-4, performed a cyclic tension-compression test, and developed a finite element model based on the experimental data that can be utilized in predicting the lifetime assessment of PCBs under thermal load. The effect of indentation depth and hold time on the mechanical properties of woven glass/epoxy substrate which is being used in PCBs was investigated by Misrak et al. [24]. According to their findings, the modulus of elasticity, hardness, and creep time greatly depends on the surface roughness, location, maximum indentation load, and hold time. Wang et al. [25] investigated the drop-impact behavior of multilayer PCBs for four different types of material models and they were isotropic model, orthotropic model, multi-layer unidirectional model, and multi-layer fill-warp model and they found that the multi-layer fill-warp model predicts the accurate results when compared to the experimental results.

The reliability of solder joints in a PCB is studied by Gleichauf et al. [26] under combined cyclic thermal and bending loads where they have developed a Finite Element Model (FEM) to predict the bending strain in a PCB. The interfacial reliability of the potting-PCB interface is investigated by Lall et al. [27] after long-term exposure of the PCB at high temperatures. Zhang et al. [28] developed a computational model to predict the plastic deformation on inner copper layers in a PCB under cyclic bending load and suggested that the plasticity of the inner copper layer should be accounted for in predicting the lifetime of a PCB. The mode-I fracture toughness of the epoxy/PCB interface is investigated by several researchers [29–31] either experimentally or using Cohesive Zone Modeling (CZM) approach to predict the mode-I fracture toughness. Oliveira et al. [32] developed a FEM model which can predict the bending strain in a PCB during In Circuit Test (ICT) which can be utilized to design ICT test fixtures to prevent any damage to PCBs.

From the above discussion, it is clear that various researchers have studied different aspects of PCBs mostly the warpage caused by thermomechanical loading, or utilized deep learning methods to predict the thermomechanical behavior of PCBs. However, there is a limited amount of research on the pure bending of PCBs under mechanical load, which is crucial since PCBs must support other components mounted on them, leading to bending. Therefore in this paper, the effect of FR-4 ply orientation and lamina thickness variation on the bending properties of multi-layer PCBs is investigated using commercially available finite element analysis software. A three-point bending test was simulated and the model was validated using experimental results obtained from the literature. The bending stiffness, maximum displacement, equivalent modulus of elasticity, and von-Mises stress were investigated for various ply orientations and lamina thicknesses to develop a comprehensive understanding. The results were found to be promising for application in the PCB manufacturing industries.

2. Computational modeling

2.1. Materials

PCBs are usually made of glass fiber-reinforced epoxy composites sandwiched (commercially known as FR-4) with copper-clad laminates (CCL) between copper foils. The benefit of FR4 is that it has an excellent resistance-to-weight ratio. It does not absorb water, possesses high mechanical and fire retardant properties, and serves as an effective insulator in both dry and wet conditions. Its low cost makes it suitable for small-series PCB fabrication or electrical prototyping. The mechanical properties of the FR-4 layer and copper are given in Table 1. The FR-4 layer consists of a cross-ply with a 0° and a 90° ply. The volume fraction of fiber in 0° ply is 0.52 and in 90° ply is 0.40.

2.2. Modeling conditions

Two dimensional deformable part with a length of 50 mm and width of 30 mm as shown in Fig. 1 (a) was modeled using commercially available finite element software Abaqus version 6.17. Three-point bending test was simulated with a span length of 46 mm and a uniformly distributed load of 99.3 N was applied along the centerline of the specimen throughout the width as shown in Fig. 1 (b). The value of the load was taken from Ref. [2] since they found that the average load for the 5 mm deflection of the specimens is 99.3 N. A linear-elastic analysis was performed with two roller supports and the load was applied with a loading roller at the center of the specimen (refer to Fig. 1 (b)).

S4R elements which are 4-node quadrilateral shell elements were used to model the specimen because of their suitability for thin plates [33]. Fig. 2 (a) shows the typical mesh on the model with uniform shell elements. Mesh sensitivity analysis was performed to ensure that the results are independent of the mesh size. Fig. 2 (b) shows the mesh sensitivity analysis graph, where von-Mises stress and deflection were plotted against the number of elements. It is observed from this figure that the von-Mises stress and the deflection both increases initially with the increase in the number of elements. However, the von-Mises stress and deflection becomes constant at 9450 number of elements and the results do not change with further increasing the number of elements in the model. Since after 9450 number of elements both von-Mises stress and deflection remains unchanged, it can be said that the results generated from the model are independent of the mesh size. So, it was used for further analysis; in this case, the global mesh size was 0.4 mm.

Table 1
Material Properties [2].

Material	E_1 (MPa)	E_2 (MPa)	G_{12} (MPa)	ν_{12}	ρ (kg/m^3)
FR-4	22000	22000	3500	0.28	1940
Copper	103000	103000	39700	0.33	8940

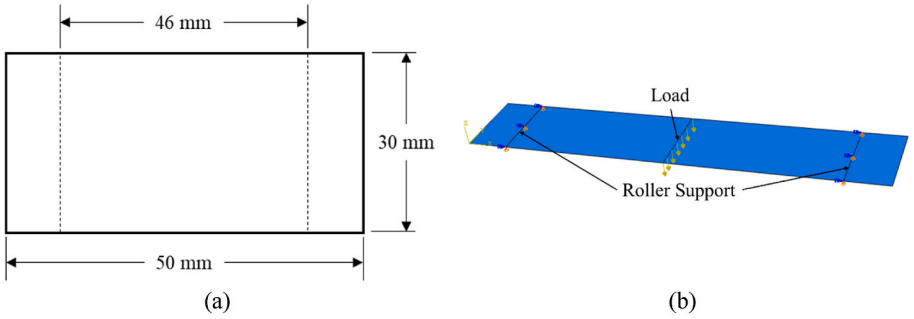

Fig. 1. (a) Schematic diagram of the model, and (b) load and boundary conditions.

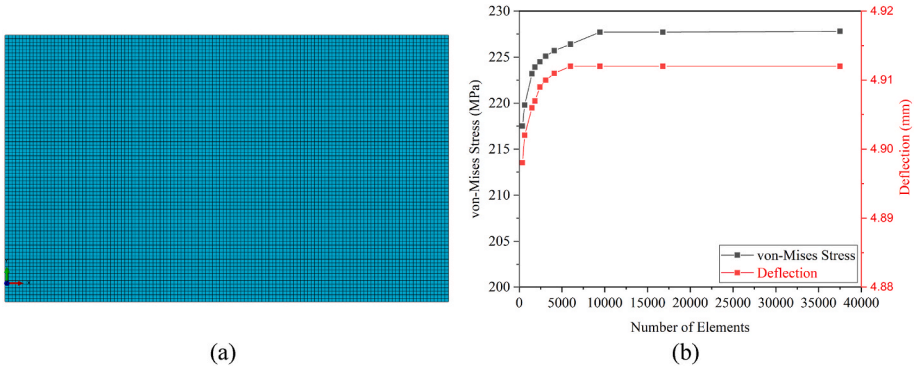

Fig. 2. (a) Typical mesh with shell elements, and (b) mesh sensitivity analysis.

To investigate the effect of ply orientations, seven different orientations were considered and they are identified as O1 to O7. Since the copper foil is isotropic, the orientation does not have any effect, the orientations were changed only for the FR-4 as shown in Table 2. Among these models, model O1 represents the cross-ply laminate while the other models are angle-ply laminates.

To investigate the effect of lamina thickness, eight different lamina thicknesses were considered in this investigation as listed in Table 3. Here, the models were identified as T1, T2, T3, etc. The total thickness of all the models was kept constant and only the individual lamina thicknesses were varied.

Table 2
Ply orientations of different models considered in the analysis.

Material Type	Ply Orientations						
	O1	O2	O3	O4	O5	O6	O7
FR-4	0	0	-45	45	45	45	90
FR-4	90	90	45	-45	-45	-45	0
Copper Foil	0	0	0	0	0	0	0
FR-4	0	45	0	0	45	90	45
FR-4	90	-45	90	90	-45	0	-45
Copper Foil	0	0	0	0	0	0	0
FR-4	0	0	0	45	45	90	45
FR-4	90	90	90	-45	-45	0	-45
CCL	0	0	0	0	0	0	0
FR-4	90	45	0	90	45	45	90
FR-4	90	45	0	90	45	45	90
CCL	0	0	0	0	0	0	0
FR-4	90	90	90	-45	-45	0	-45
FR-4	0	0	0	45	45	90	45
Copper Foil	0	0	0	0	0	0	0
FR-4	90	-45	90	90	-45	0	-45
FR-4	0	45	0	0	45	90	45
Copper Foil	0	0	0	0	0	0	0
FR-4	90	90	-45	-45	-45	-45	0
FR-4	0	0	45	45	45	45	90

3. Results and discussions

3.1. Model validation

Numerical simulation was performed following the materials and methods described in the study by Li et al. [2], and the load-displacement response obtained from the simulation is compared with the experimental results as shown in Fig. 3. It is seen that the load increases linearly with increasing deflection as expected since a linear elastic simulation was performed. This figure demonstrates that the load-displacement response obtained from our simulation closely aligns with the experimental findings of Li et al. [2]. However, a slight deviation is observed in the displacement range of 1.5 mm–3.5 mm. This discrepancy can be attributed to the nonlinearity in the load-displacement response since their results were based on experimental data, while our current analysis assumed linear elasticity.

3.2. Effect of ply orientation

In this section, we present the results of the load-deflection response and bending stiffness analysis for various ply orientations. The aim is to assess the impact of different ply orientations on the mechanical properties of the composite laminate. The load-deflection response is linear for all ply orientations, as depicted in Fig. 4 (a). The slopes of the load-deflection curves provide insights into the stiffness variations among the models. Model O1 exhibits a higher slope, indicating greater stiffness, whereas model O5 shows a lower slope, suggesting reduced stiffness. This observation aligns with the intuitive relationship between slope and stiffness in load-deflection curves (Fig. 4(b)) as well. Model O1 serves as the baseline and the bending stiffness of this model is 20.23 N/mm. The stiffness of model O1 is 12.16% greater than model O5 that is showing the minimum stiffness. Model O3 and O6 show similar stiffness despite the variation in the ply orientation. Model O2 shows a decrease in stiffness by 3.16% compared to the base model.

Other than bending stiffness, the equivalent modulus of elasticity is

Table 3
Variation of lamina thicknesses.

Lamina	Lamina Thickness (mm)							
	T1	T2	T3	T4	T5	T6	T7	T8
FR-4[a]	0.04	0.06	0.05	0.04	0.04	0.03	0.04	0.06
Copper Foil	0.012	0.012	0.012	0.012	0.012	0.012	0.012	0.012
FR-4[a]	0.04	0.06	0.05	0.04	0.04	0.03	0.04	0.06
Copper Foil	0.012	0.012	0.012	0.012	0.012	0.012	0.012	0.012
FR-4[a]	0.11	0.09	0.12	0.10	0.11	0.13	0.08	0.06
CCL	0.1	0.09	0.065	0.11	0.09	0.09	0.145	0.145
FR-4[a]	0.11	0.09	0.12	0.11	0.13	0.13	0.08	0.04
CCL	0.10	0.09	0.065	0.11	0.09	0.09	0.145	0.145
FR-4[a]	0.11	0.09	0.12	0.10	0.11	0.13	0.08	0.06
Copper Foil	0.012	0.012	0.012	0.012	0.012	0.012	0.012	0.012
FR-4[a]	0.04	0.06	0.05	0.04	0.04	0.03	0.04	0.06
Copper Foil	0.012	0.012	0.012	0.012	0.012	0.012	0.012	0.012
FR-4[a]	0.04	0.06	0.05	0.04	0.04	0.03	0.04	0.06
Volume Fraction of CCL	0.27	0.24	0.18	0.30	0.24	0.24	0.39	0.39

[a] Each FR-4 consists of two equal-thickness layers of glass fiber reinforced epoxy composite.

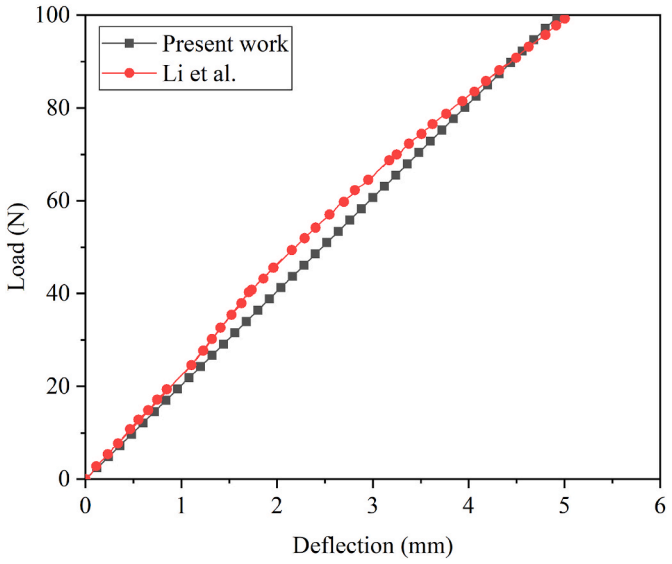

Fig. 3. Comparison of the load-deflection response of present work with [2].

also calculated and compared. The following equation [33] is used to calculate the equivalent modulus of elasticity-

$$E_x = \frac{F}{v}\cdot\frac{l^3}{48 I_z} \tag{1}$$

Where, E_x (MPa) is the equivalent modulus of elasticity, F (N) is the bending force, v (mm) is the midspan deflection, l (mm) is the span length and I_z (mm^4) is moment of inertia with respect to the z-axis.

Similar to the stiffness results, the calculated equivalent modulus of elasticity for O1 is the maximum, and for O5 it is minimum as shown in Fig. 4 (b). The equivalent modulus of elasticity for O1 is 26.62 GPa and for O5 is 23.39 GPa which is 12.13% lower than the base model. It is clear from Fig. 4 (b) that the bending stiffness and equivalent modulus of elasticity are significantly affected by the ply orientation and stacking sequence. Further analysis on the effect of ply orientation on the stiffness and equivalent modulus of elasticity is given at the later stage in this section in relation with other properties of the laminate.

The contour of the displacement and von-Mises stress along the thickness direction (i.e. z-axis) for different ply orientations are shown in Figs. 5 and 6 respectively. It can be observed from Fig. 5 that the displacement for model O5 is maximum and it is minimum for O1 for the same fixed load of 99.3 N. The displacement of O5 is 13.88% greater than O1 as listed in Table 4.

The von-Mises stress serves as a critical parameter for failure assessment. When von-Mises stress surpasses the material's yield strength, it initiates plastic deformation, and if this stress continues to escalate, eventual material failure occurs. While the current analysis assumes linear elastic behavior, the examination of von-Mises stress across various models provides a qualitative understanding of potential variations in failure tendencies under identically applied loads. Among the models, O7 reports the highest maximum von-Mises stress, while O3 exhibits the lowest. Specifically, the maximum von-Mises stress for O7 exceeds that of the baseline model O1 by 8.50%, whereas for O3, it is notably 19.33% lower than O1.

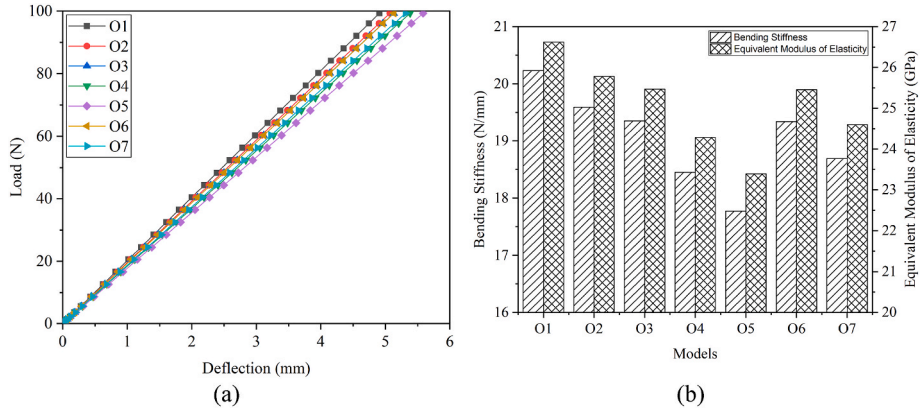

Fig. 4. (a) Load-deflection response and (b) Bending stiffness and equivalent modulus of elasticity for different ply orientations.

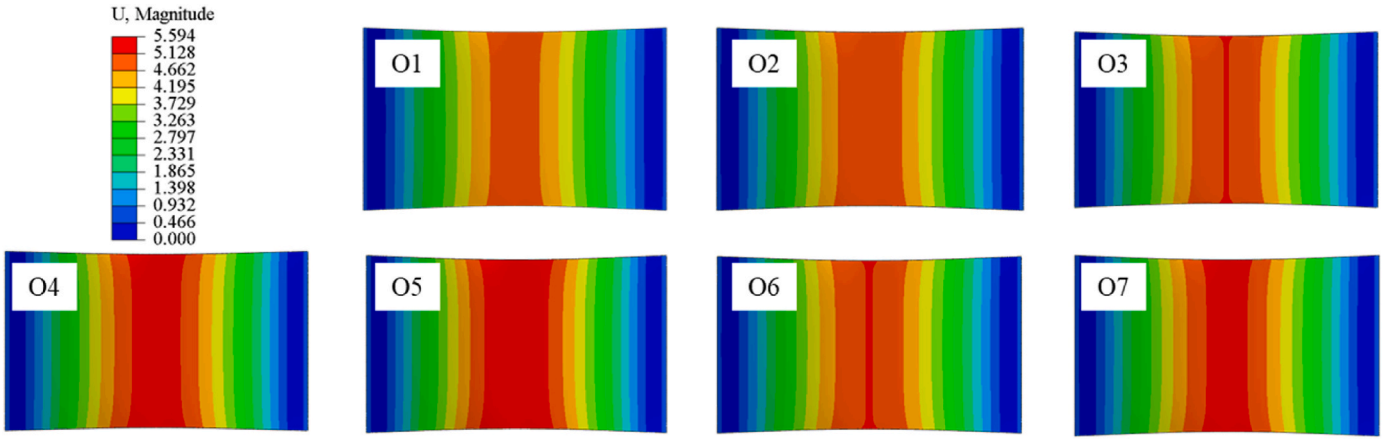

Fig. 5. Displacement along the thickness direction for different ply orientations.

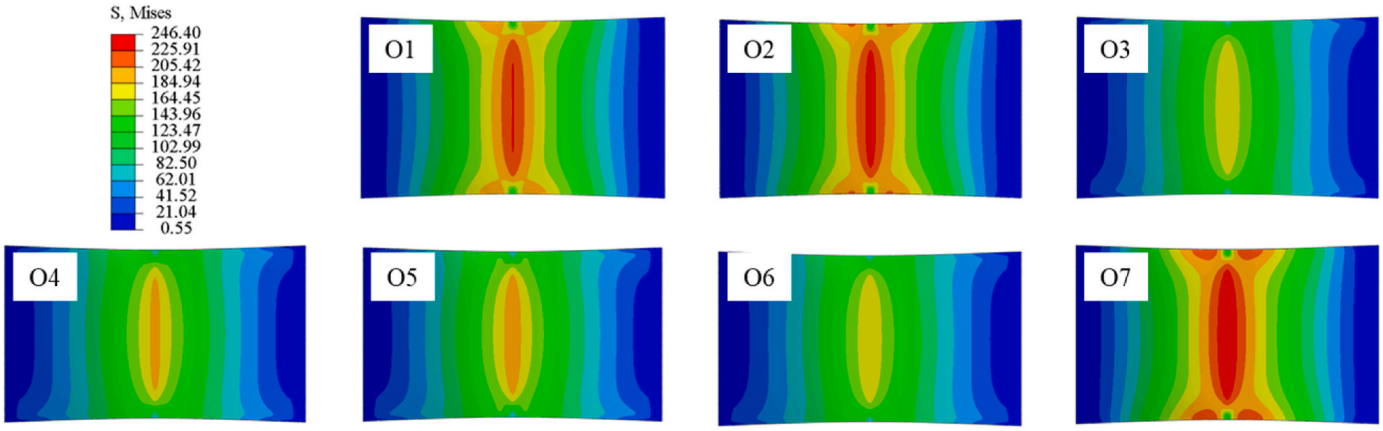

Fig. 6. Von-Mises stress distribution for different ply orientations.

Table 4
Comparison of bending properties of all the models.

Models	Stiffness (N/mm)	Percentage Change (%)	Modulus (GPa)	Percentage Change (%)	Displacement (mm)	Percentage Change (%)	von-Mises Stress (MPa)	Percentage Change (%)
O1	20.23	–	26.62	–	4.912	–	227.10	–
O2	19.59	-3.16	25.78	-3.16	5.073	3.28	234.90	3.43
O3	19.35	-4.35	25.47	-4.32	5.135	4.54	183.20	-19.33
O4	18.45	-8.80	24.28	-8.79	5.389	9.71	192.40	-15.28
O5	17.77	-12.16	23.39	-12.13	5.594	13.88	199.70	-12.07
O6	19.34	-4.40	25.46	-4.36	5.137	4.58	183.30	-19.29
O7	18.69	-7.61	24.60	-7.59	5.316	8.22	246.40	8.50

Analysis of Table 4 reveals a similarity in the bending properties of models O3 and O6. Notably, the distinctions between these models are twofold: firstly, the substitution of two 0° laminas in the central FR-4 layer of O3 with 45° laminas, and secondly, a modification in the ply orientation within the remaining FR-4 layers, excluding the bottommost one. These observations collectively suggest that variations in laminar orientations within the FR-4 layers have a limited impact on the overall bending properties.

Further scrutiny of Table 4 reveals a slight increase in the maximum von-Mises stress for O2 compared to O1, while model O7 demonstrates a notably elevated maximum von-Mises stress in comparison to both models O1 and O2. The stiffness is slightly reduced in model O2 and significantly reduced in model O7. For model O2, three FR-4 layers containing angle plies were introduced by replacing three internal FR-4 cross ply of layers keeping two outer FR-4 layers unchanged. For model O7, four FR-4 angle ply layers were introduced by replacing the cross plies, middle FR-4 layer was left unchanged, and the ply orientation at the outer two FR-4 layers were altered. Note that the bending properties are not significantly affected by altering the orientation of intra FR-4 laminas as discussed earlier and it is established in the literature that the angle plies offer less stiffness compared to cross plies. So, it is evident that the introduction of angle plies in the internal FR-4 layers is the main reason for reduced stiffness (see Fig. 4(b) and Table 2) because of the lower stiffness of the angle plies. The same reason applies to the higher maximum von-Mises stress in models O2 and O7 because the stiffness difference between copper foils and FR-4 layers with angle plies increases significantly which causes a higher stress jump between these two layers. Model O5 shows minimum stiffness (see Fig. 4(b)) and Table 4) because all FR-4 layers consist of angle plies with lower stiffness. Models O4 and O7 have the same number of FR-4 angle ply layers but in model O4, two of the angle ply-based FR-4 layers were placed at two outermost locations in the laminate which caused a decrease in

stiffness compared to model O7. Because the stiffer layers must be placed at the outer sides of the laminate to achieve the highest overall stiffness of a laminate [34]. For the same reason, the maximum von-Mises stress in O4 is seen to be lower than that of O7 (see Table 4) despite the same number of angle ply-based FR-4 layers. The maximum von-Mises stress in models O3 and O6 is because of the placement of less stiff angle ply-based FR-4 layers at the outer side causing comparatively lower overall stiffness of the laminate and higher displacement without a significant increase in stress jump between copper foils and the angle ply-based FR-4 layers.

Based on the bending properties considered in the analysis, it can be said that O1 represents the best ply orientation because the bending stiffness and equivalent modulus of elasticity are maximum for this model and the displacement is minimum. For a printed circuit board, higher bending stiffness or lower bending deflection is desired [2]. The introduction of angle ply has a negative effect on the bending stiffness, modulus, and maximum displacement but it has improved the von-Mises stress. So, models O3 and O6 can also be considered for application in printed circuit boards because of their lower von-Mises stress (19.33% and 19.29% respectively compared to model O1) by compromising the stiffness by 4.35% and 4.40% respectively (see Table 4).

3.3. Effect of lamina thickness

The effect of ply orientation on the bending properties of PCB is discussed in section 3.2 and it is found that model O1 represents the optimum ply orientation in terms of the laminate stiffness. So, for orientation O1, the thicknesses of the FR-4 and CCL are varied to investigate the effect of lamina thickness. Here, eight variations of lamina thicknesses were considered as reported in Table 3. Fig. 7 (a) shows the bending stiffness and equivalent modulus of elasticity for different lamina thicknesses. It is observed that both the bending stiffness and the equivalent modulus of elasticity for T7 are higher compared to all the models. The bending stiffness and equivalent modulus of elasticity are 11.72% and 11.80% higher compared to the base model as shown in Table 5. For the comparison purpose in this case T1 model is considered as the base model which is the same model in the previous section i.e. O1.

Model T2, T5, and T6 consist of the same volume fraction of CCLs in the laminate through the cross section but model T2 shows lower stiffness compared to the other two. The thickness of the outer two layers of FR-4 is reduced in models T5 and T6 while the thickness of the FR-4 layers adjacent to the CCLs is increased. As a result of this modification, the stiffer copper foil layers have moved away from the centerline of the specimen. This accounts for the increased stiffness observed in T5 and T6 as compared to T2, aligning with the principles of the sandwich theory, which posits that higher sandwich stiffness is achieved when the stiffer layer is positioned away from the centerline.

Comparing the models T7 and T8, for the same volume fraction of CCLs (0.39), it is observed that T8 has lower stiffness than T7. It is also due to the movement of stiffer copper foil layers towards the center for model T8 because of the increase in the thickness of the outer FR-4 layers. Despite the decrease in volume fraction of CCL for model T5, the stiffness loss of model T5 compared to model T7 is insignificant because of the movement of the CCLs away from the centerline of the specimen. Similarly, model T6 displays a higher stiffness than model T1 due to the shifting of outer copper foil layers away from the centerline, although the volume fraction of CCL in T5 is lower than T1. The reasons for the lowest stiffness of model T3 are firstly, the increase in outer FR-4 layers which shifted the stiffer copper foil layer towards the centerline, and secondly, the reduction of the volume fraction of CCLs. The higher stiffness of models T4 and T7 compared to T1 is mainly due to the increased volume fraction of CCL. The model T8 shows a decrease in stiffness compared to T1 despite a significant increase in volume fraction of CCL because of the movement of the copper foil layers towards the centerline of the specimen.

If the outer four layers of the laminate are kept constant which is the case for models T1, T4, T5 and T7 (see Table 3) the stiffness of the composite is highly dependent on the volume fraction of CCL in the composite as shown in Fig. 7 (b). It is seen that the stiffness of the composite increases linearly with increasing the volume fraction of CCL in the composite with a very high correlation coefficient $R^2 = 0.9849$. It indicates that the position of the layers (i.e. stacking sequence) adjacent to the centerline of the composite cross section does not have significant impact on the stiffness of the laminate.

So, it can be deduced that the variation of thickness of various layers in the laminate causes changes in two parameters i.e. the volume fraction of the constituent laminas and the distance of laminas from the center of the specimen. These two changes significantly affect the bending properties of the composite laminate. The best result can be obtained by compromising between these two changes. For example, for a constant volume fraction of CCL in the composite, the layer thickness should be adjusted in such a way that the copper foil layers and the CCLs are placed away from the centerline as much as possible to achieve a higher stiffness. On the other hand, for a fixed position of the outer layers (i.e. two copper foil layers and two outer FR-4 layers), the volume fraction of CCL may be increased to obtain higher bending stiffness.

The displacement contours for all the models are shown in Fig. 8 and it is observed that the displacement is maximum for model T3 and it is minimum for model T7. The maximum displacement for model T3 is 19.48% higher while the maximum displacement for model T7 is 10.57% lower than the base model as reported in Table 5. The von-Mises stress distribution is shown in Fig. 9 for different thicknesses and the same trend is also observed i.e. the von-Mises stress for model T3 is

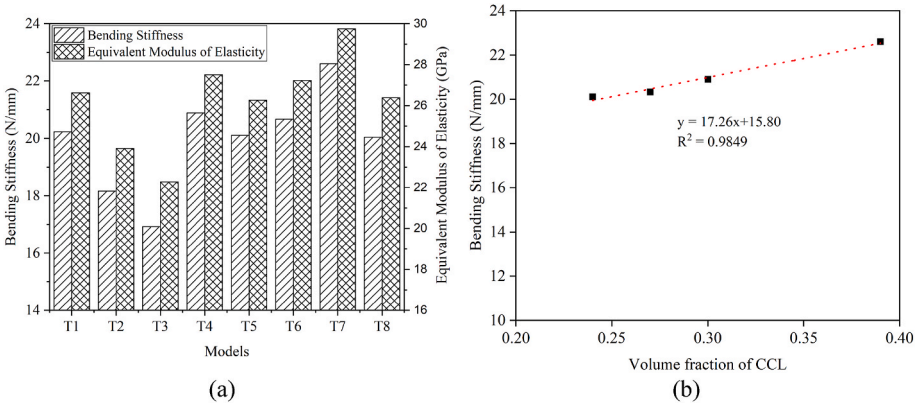

Fig. 7. (a) Bending stiffness and equivalent modulus of elasticity for different lamina thicknesses (b) The stiffness of the composites as a function of the volume fraction of CCL.

Table 5
Comparison of bending properties of all the models.

Models	Stiffness (N/mm)	Percentage Change (%)	Modulus (GPa)	Percentage Change (%)	Displacement (mm)	Percentage Change (%)	Von-Mises Stress (MPa)	Percentage Change (%)
T1	20.23	–	26.62	–	4.912	–	227.08	–
T2	18.16	-10.23	23.91	-10.18	5.468	11.32	252.96	11.40
T3	16.92	-16.36	22.28	-16.30	5.869	19.48	265.98	17.13
T4	20.89	3.26	27.50	3.31	4.754	-3.22	219.74	-3.23
T5	20.11	-0.59	26.26	-1.35	4.937	0.51	228.21	0.50
T6	20.67	2.17	27.22	2.25	4.803	-2.22	222.02	-2.23
T7	22.60	11.72	29.76	11.80	4.393	-10.57	203.03	-10.59
T8	20.04	-0.94	26.38	-0.90	4.956	0.90	229.17	0.92

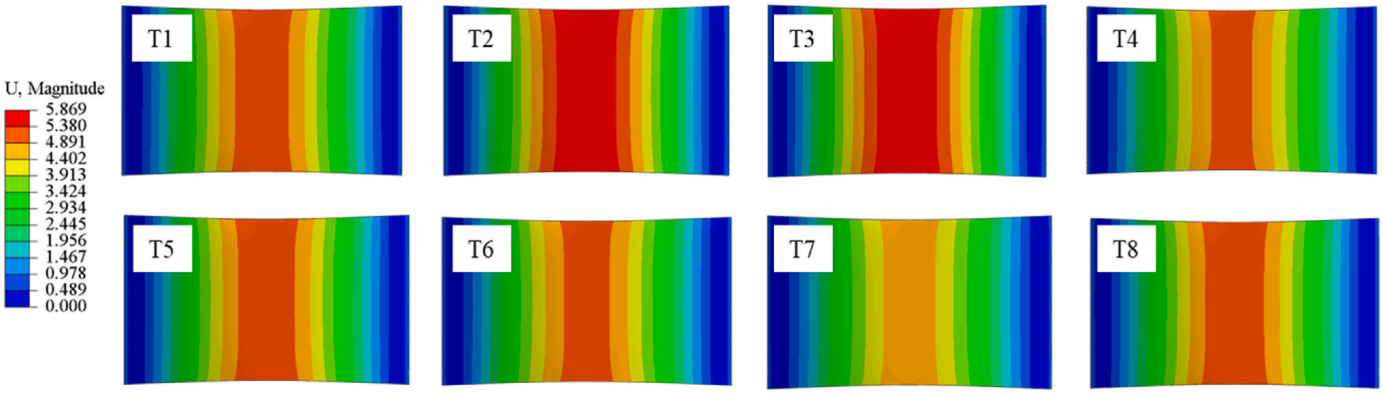

Fig. 8. Displacement along the thickness direction for different lamina thicknesses.

17.13% higher and for model T7 it is 10.59% lower than the base model.

From the above discussion, it is evident that model T7 is found to be the best in terms of both stiffness and maximum von-Mises stress among the eight different lamina thicknesses considered in this analysis.

3.4. Optimum ply orientation and lamina thickness

From section 3.2 it is found that model O1 represents the best ply orientations based on the laminate stiffness and model T7 represents the best lamina thicknesses as discussed in section 3.3. However, at this stage, we cannot conclude that O1 orientation and T7 thicknesses are best as other orientations for T7 thickness were not considered. It might be possible to get better bending properties for T7 thickness and other orientations (other than O1). In order to investigate that, other orientations with T7 lamina thicknesses are considered as well and the possible models are named as O1T7, O2T7, and so on, and in this case, O1T7 serves as the base model for comparison.

Fig. 10 shows the bending stiffness for different ply orientations and thicknesses. It is observed from this figure that the bending stiffness is maximum for model O1T7. The bending stiffness for this model is found to be 22.60 N/mm as shown in Table 6. Table 6 reports the bending stiffness, modulus, maximum displacements and maximum von-Mises stress for T7 lamina thicknesses and other possible orientations. It is found from this table that the bending stiffness and equivalent modulus of elasticity are maximum for model O1T7 and the displacement is minimum for this model which indicates that O1 ply orientation with T7 thickness distribution is the best in terms of bending stiffness among all the orientations and thickness distributions considered in this work.

The von-Mises stress is found to be minimum for models O3T7 and O6T7. So, again, models O3 and O6 with T7 thickness distribution may also be considered for application in printed circuit boards by sacrificing the laminate bending stiffness by 3.85% and 3.45% respectively. This would also increase the life of the laminate because the lower the von-Mises stress higher the lifetime of the structure.

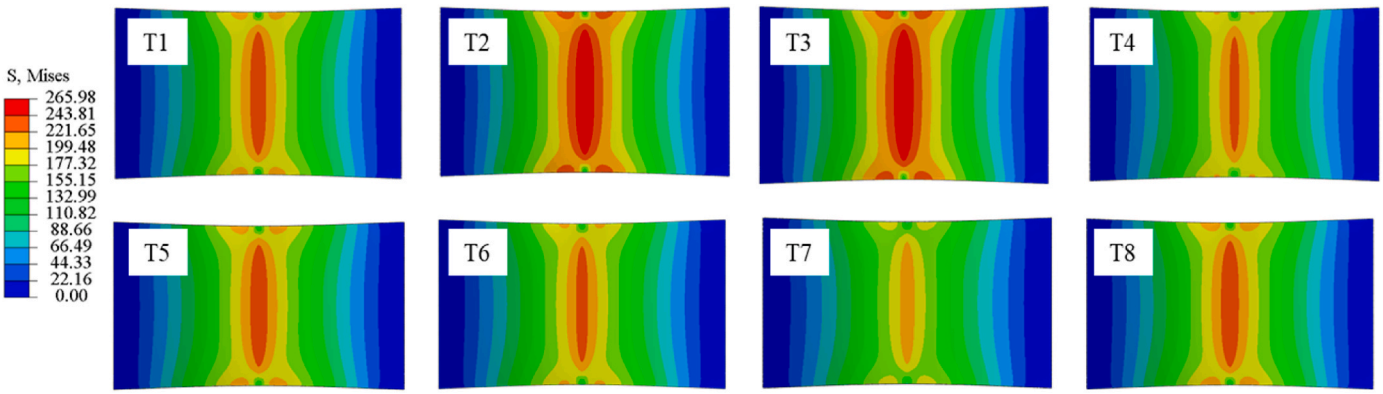

Fig. 9. Von-Mises stress distribution for different lamina thicknesses.

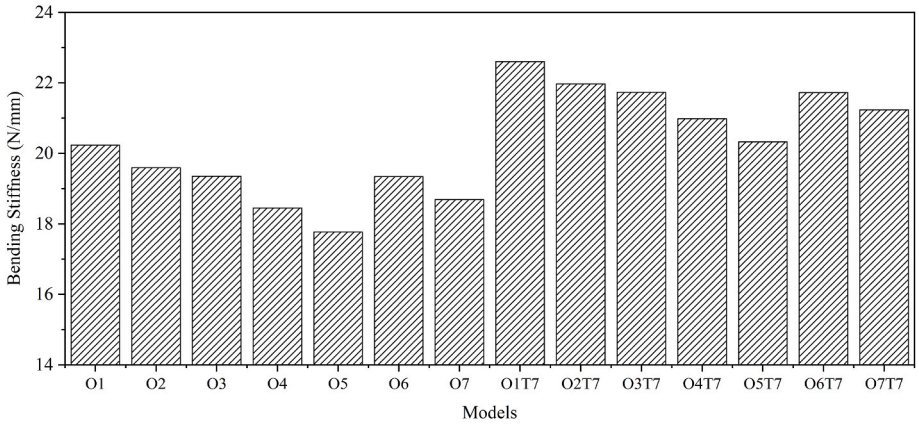

Fig. 10. Comparison of bending stiffness of different models.

Table 6
Comparison of bending properties of T7 models with different ply orientations.

Models	Stiffness (N/mm)	Percentage Change (%)	Modulus (GPa)	Percentage Change (%)	Displacement (mm)	Percentage Change (%)	Von-Mises Stress (MPa)	Percentage Change (%)
O1T7	22.60	–	29.76	–	4.393	–	203.03	–
O2T7	21.97	-2.79	28.93	-2.79	4.520	2.89	209.14	3.01
O3T7	21.73	-3.85	28.62	-3.83	4.570	4.03	162.96	-19.74
O4T7	20.98	-7.17	27.63	-7.16	4.733	7.74	168.88	-16.82
O5T7	20.32	-10.09	26.76	-10.08	4.887	11.25	174.38	-14.11
O6T7	21.72	-3.45	28.61	-3.86	4.571	4.05	162.99	-19.72
O7T7	21.23	-6.06	27.95	-6.08	4.678	6.49	216.61	6.69

4. Conclusions

The aim of this research was to investigate the effect of ply orientation and lamina thickness on the bending properties of multi-layer PCBs. Seven different ply orientations and eight different lamina thickness distributions were considered in this investigation. The following points summarize the outcome of this research-

- The ply orientation significantly affects the bending properties of the multi-layer PCBs such that the introduction of angle ply by replacing the cross ply decreases the bending stiffness but the improvement in maximum von-Mises stress is evident.
- The bending stiffness and equivalent modulus of elasticity for model O1 are maximum compared to all other ply orientations considered. However, models O3 and O7 show comparable stiffness and equivalent modulus of elasticity with improved von-Mises stress.
- The variation of lamina thicknesses keeping the overall thickness of the laminate constant changes two parameters in the laminate (i.e. the volume fraction of the constituent laminas and the distance of laminas from the center of the specimen) which affects the bending properties of the multi-layer PCBs. The laminate stiffness can be significantly increased by increasing the volume fraction of stiffer laminas and placing the stiffer laminas away from the centroid axis of the laminate.
- The bending stiffness and equivalent modulus of elasticity for model T7 are maximum which are respectively 11.72% and 11.80% greater than the base model. On the other hand, the maximum deflection for model T7 is 10.57% lower than the base model.
- The bending stiffness and equivalent modulus of elasticity for model O1T7 are maximum (20.60 N/mm and 29.76 GPa respectively) and the maximum deflection is minimum among all the variations considered in this research.
- Model O1T7 exhibits the best bending performances in terms of stiffness and the maximum deflection among all the models but a compromise of less than 5% in bending stiffness could lead to a multi-layer PCB (models O3T7 and O6T7) with better von-Mises stress and longer lifetime.

Declaration of competing interest

The authors declare that they have no known competing financial interests or personal relationships that could have appeared to influence the work reported in this paper.

References

[1] V.K. Yaddanapudi, et al., Validation of new approach of modelling traces by mapping mechanical properties for a printed circuit board mechanical analysis, in: 2015 IEEE 17th Electronics Packaging and Technology Conference (EPTC), IEEE, 2015.
[2] L. Li, et al., Finite element modeling and simulation for bending analysis of multi-layer printed circuit boards using woven fiber composite, J. Mater. Process. Technol. 201 (1–3) (2008) 746–750.
[3] U. Rahangdale, et al., Mechanical characterization of RCC and FR4 laminated PCBs and assessment of their board level reliability, in: 2017 16th IEEE Intersociety Conference on Thermal and Thermomechanical Phenomena in Electronic Systems (ITherm), IEEE, 2017.
[4] P. Hutapea, J.L. Grenestedt, Effect of temperature on elastic properties of woven-glass epoxy composites for printed circuit board applications, J. Electron. Mater. 32 (2003) 221–227.
[5] S. Ramdas, et al., Impact of immersion cooling on thermo-mechanical properties of PCB's and reliability of electronic packages, in: International Electronic Packaging Technical Conference and Exhibition, American Society of Mechanical Engineers, 2019.
[6] S.-W. Kim, et al., Simulation of warpage during fabrication of printed circuit boards, IEEE Trans. Compon. Packag. Manuf. Technol. 1 (6) (2011) 884–892.
[7] M. Shevchuk, et al., Prediction of thermo-mechanical properties of PCB conductive layers using convolutional neural networks, in: 2023 24th International Conference on Thermal, Mechanical and Multi-Physics Simulation and Experiments in Microelectronics and Microsystems (EuroSimE), IEEE, 2023.
[8] S. Stoyanov, C. Bailey, Deep learning modelling for composite properties of pcb conductive layers, in: 2022 23rd International Conference on Thermal, Mechanical and Multi-Physics Simulation and Experiments in Microelectronics and Microsystems (EuroSimE), IEEE, 2022.
[9] K. Gholami, F. Ege, R. Barzegar, Prediction of composite mechanical properties: integration of deep neural network methods and finite element analysis, J. Compos. Sci. 7 (2) (2023) 54.

[10] C. Rao, Y. Liu, Three-dimensional convolutional neural network (3D-CNN) for heterogeneous material homogenization, Comput. Mater. Sci. 184 (2020), 109850.
[11] D.-H. Kim, et al., Warpage simulation of a multilayer printed circuit board and microelectronic package using the anisotropic viscoelastic shell modeling technique that considers the initial warpage, IEEE Trans. Compon. Packag. Manuf. Technol. 6 (11) (2016) 1667–1676.
[12] S.-J. Joo, et al., Investigation of multilayer printed circuit board (PCB) film warpage using viscoelastic properties measured by a vibration test, J. Micromech. Microeng. 25 (3) (2015), 035021.
[13] D.-H. Kim, et al., Anisotropic viscoelastic shell modeling technique of copper patterns/photoimageable solder resist composite for warpage simulation of multi-layer printed circuit boards, J. Micromech. Microeng. 25 (10) (2015), 105016.
[14] A.S. Halvi, et al., Simulation of PWB warpage during fabrication and due to reflow, in: The Ninth Intersociety Conference on Thermal and Thermomechanical Phenomena in Electronic Systems (IEEE Cat. No. 04CH37543), IEEE, 2004.
[15] J.L. Grenestedt, P. Hutapea, Influence of electric artwork on thermomechanical properties and warpage of printed circuit boards, J. Appl. Phys. 94 (1) (2003) 686–696.
[16] C.-S. Lau, et al., A numerical technique to evaluate warpage behavior of double sided rigid-flex board assemblies during reflow soldering process, in: 2020 IEEE 70th Electronic Components and Technology Conference (ECTC), IEEE, 2020.
[17] S.J. Oon, et al., Warpage studies of printed circuit boards with Shadow Moiré and simulations, in: 2018 IEEE 38th International Electronics Manufacturing Technology Conference (IEMT), IEEE, 2018.
[18] Q. Nguyen, et al., A simulation study on SSD PCB warpage during reflow: from understanding to improvement, in: 2023 22nd IEEE Intersociety Conference on Thermal and Thermomechanical Phenomena in Electronic Systems (ITherm), IEEE, 2023.
[19] T.-I. Lee, et al., Effect of anisotropic thermo-elastic properties of woven-fabric laminates on diagonal warpage of thin package substrates, Compos. Struct. 176 (2017) 973–981.
[20] M. Lee, Finite element modelling of printed circuit boards (PCBs) for structural analysis, Solder. Surf. Mt. Technol. 10 (3) (1998) 12–17.
[21] E.T. Haugan, P. Dalsjø, Characterization of the Material Properties of Two FR4 Printed Circuit Board Laminates, 2014.
[22] V.S. Chippalkatti, et al., Estimation of equivalent mechanical properties of multi-layered PCBs based on FEA, vibration testing and analytical calculation, in: AIP Conference Proceedings., AIP Publishing, 2021.
[23] K. Fellner, et al., Determination of cyclic mechanical properties of thin copper layers for PCB applications, in: 2014 15th International Conference on Thermal, Mechanical and Mulit-Physics Simulation and Experiments in Microelectronics and Microsystems (EuroSimE), IEEE, 2014.
[24] A. Misrak, et al., Characterization of mechanical properties and creep behavior of woven glass/epoxy substrates by Nanoindentation, J. Microelectronics and electron. packag. 15 (2) (2018) 95–100.
[25] Y. Wang, et al., Modeling and simulation for a drop-impact analysis of multi-layered printed circuit boards, Microelectron. Reliab. 46 (2–4) (2006) 558–573.
[26] J. Gleichauf, Y. Maniar, S. Wiese, Reliability testing of solder joints under combined cyclic thermal and bending load for automotive applications, Microelectron. Reliab. 139 (2022), 114751.
[27] P. Lall, A.R.R. Pandurangan, K. Blecker, Evolution of potting-PCB interfacial reliability after long term high temperature operation, in: International Electronic Packaging Technical Conference and Exhibition, American Society of Mechanical Engineers, 2021.
[28] M. Zhang, et al., Investigation of the effect of PCB inner copper layer plastic deformation on solder joint fatigue simulations of mechanical cyclic bending tests, in: 2021 27th International Workshop on Thermal Investigations of ICs and Systems (THERMINIC), IEEE, 2021.
[29] P. Lall, A.R.R. Pandurangan, K. Blecker, Predictive cohesive Zone modeling for delamination at PCB-potting material interfaces under four-point bend loading with sustained high-temperature exposure, in: International Electronic Packaging Technical Conference and Exhibition, American Society of Mechanical Engineers, 2022.
[30] P. Lall, A.R.R. Pandurangan, K. Blecker, Evolution of interfacial properties under long term isothermal aging of PCB/potting compound interfacial samples under pure mode-I loading, in: 2022 21st IEEE Intersociety Conference on Thermal and Thermomechanical Phenomena in Electronic Systems (iTherm), IEEE, 2022.
[31] Akbari, S., A. Nourani, and J.K. Spelt, Cohesive zone modeling of failure in underfilled BGA-PCB assemblies under bending.
[32] R. Oliveira, et al., A systematic analysis of printed circuit boards bending during in-circuit tests, Machines 10 (2) (2022) 135.
[33] C. Cerbu, M. Botiş, Numerical modeling of the flax/glass/epoxy hybrid composite materials in bending, Procedia Eng. 181 (2017) 308–315.
[34] C. Dong, Flexural properties of symmetric carbon and glass fibre reinforced hybrid composite laminates, Composites Part C: Open Access 3 (2020), 100047.